Available online at www.sciencedirect.com
SCIENCE DIRECT®
Microelectronics Reliability 46 (2006) 1189–1198
MICROELECTRONICS RELIABILITY
www.elsevier.com/locate/microrel

A MAIC approach to TFT-LCD panel quality improvement

K.S. Chen [a], C.H. Wang [a], H.T. Chen [b,*]

[a] *Institute of Production System Engineering and Management, National Chin-Yi Institute of Technology, 35, Lane 215, Section 1, Chung San Road, Taiping, Taichung 411, Taiwan, ROC*

[b] *Department of Information Management, Chang Jung University, 396, Section 1, Chang Jung Road, Kway Jen, Tainan, Taiwan, ROC*

Received 21 July 2005; received in revised form 5 October 2005
Available online 22 November 2005

Abstract

The liquid crystal displays (LCDs) possess the most mature technology and best consuming competitiveness in the flat panel display (FPD) industries. Of all the LCDs, thin film transistor-liquid crystal display (TFT-LCD) keeps some real advantages. It is thinner, smaller and lighter than other displays and has low power consumption, low-radiation, high-contrast and high-dpi at the same time. Hence, the TFT-LCD panel is widely applied in daily electronic products, and the demand for the TFT-LCD panel increases. The product life cycle of the TFT-LCD panel is gradually getting into the mature stage, and meanwhile, Taiwan's firms face fierce competition from South Korea and Japan. Thus, at present, continual cost reduction is an all-out pursuing topic for Taiwan's panel manufacturers. If the quality and yield of the TFT-LCD panel can be effectively enhanced, the non-conforming rate and the cost of the TFT-LCD panel will be reduced. In this study, TFT-LCD panel manufacturing process is discussed, and then five critical-to-quality (CTQ) characteristics (or sub-processes) are identified and summarized. At the early stages, the assessing model of process quality index (C_{pm}) and the MAIC (i.e., measure-analyze-improve-control) approach of Six Sigma are used to measure and analyze the CTQ characteristics that make TFT-LCD panel unqualified and incapable. During the later stages, Hartley's homogeneity test and joint confidence intervals were conducted to determine the optimal parameter setting of the critical factor in TFT-LCD panel manufacturing process. By using these optimal settings, Six Sigma quality level can be achieved.

1. Manufacturing process description—TFT-LCD panel

The display is an important interface of sending message and communicating each other for people in this information technology age. The display has gradually developed from cathode ray tubes (CRTs) to flat panel displays (FPDs). Among them, liquid crystal display (LCD) technology has created a wide range of computer and consumer products that would have not been possible with CRTs. The flat and thin characteristics of LCDs make them ideal for mobile or portable applications. In addition, LCDs have some advantages, including low-radiation, high-contrast and high-dpi (dots per inch) as well as being able to operate at low voltage levels and dissipate with low heat exposure. Therefore, it has become increasingly common in a wide variety of consumer electronic devices, including cellular phones, digital cameras, LCD televisions, computer displays, and personal digital assistants (PDAs). In general, twisted

* Corresponding author. Tel.: +886 6 2785123; fax: +886 6 2785657.
E-mail address: tien7845@gmail.com (H.T. Chen).

0026-2714/$ - see front matter © 2005 Elsevier Ltd. All rights reserved.
doi:10.1016/j.microrel.2005.10.003

nematic (TN), super twisted nematic (STN) and thin film transistors (TFT) are the terms used to describe three types of LCDs. Besides, LCDs can also be divided into two types—passive matrix drive (PMD) and active matrix drive (AMD)—by different circuit-driven ways. However, the LCD panel manufacturing process is quite complicated. It combines semiconductor, photo-electricity, chemical material and sealing manufacturing process technologies. The possibility of committing mistakes is quite high in LCD panel manufacturing process. Therefore, panel makers should pay much attention on all of the manufacturing process stages and technologies. Quality defects in some stages can lead to process failure. And, most of the WIP (work in process) cannot be reworked. Finally, the later process stages or the function of final products will be affected. As a result, cost will increase. Hence, improving the process capability of LCD panel is one of the most important missions for panel manufacturers. Of all the LCDs, TFT-LCD has some of the best characteristics. It is thinner, smaller and lighter than other displays and has low power consumption, low-radiation, high-contrast and high-dpi at the same time. In this paper, the TFT-LCD manufacturing process of a medium-sized panel maker in Taiwan is provided as an illustrative example.

A TFT-LCD panel manufacturing process consists of three main stages (or processes)—*TFT array*, *cell assembly* and *module assembly process*, and at the same time, each stage consists of some sub-processes. *TFT array process* is similar to the semiconductor manufacturing process, except that transistors are fabricated on a glass substrate instead of a silicon wafer. As shown in Fig. 1,

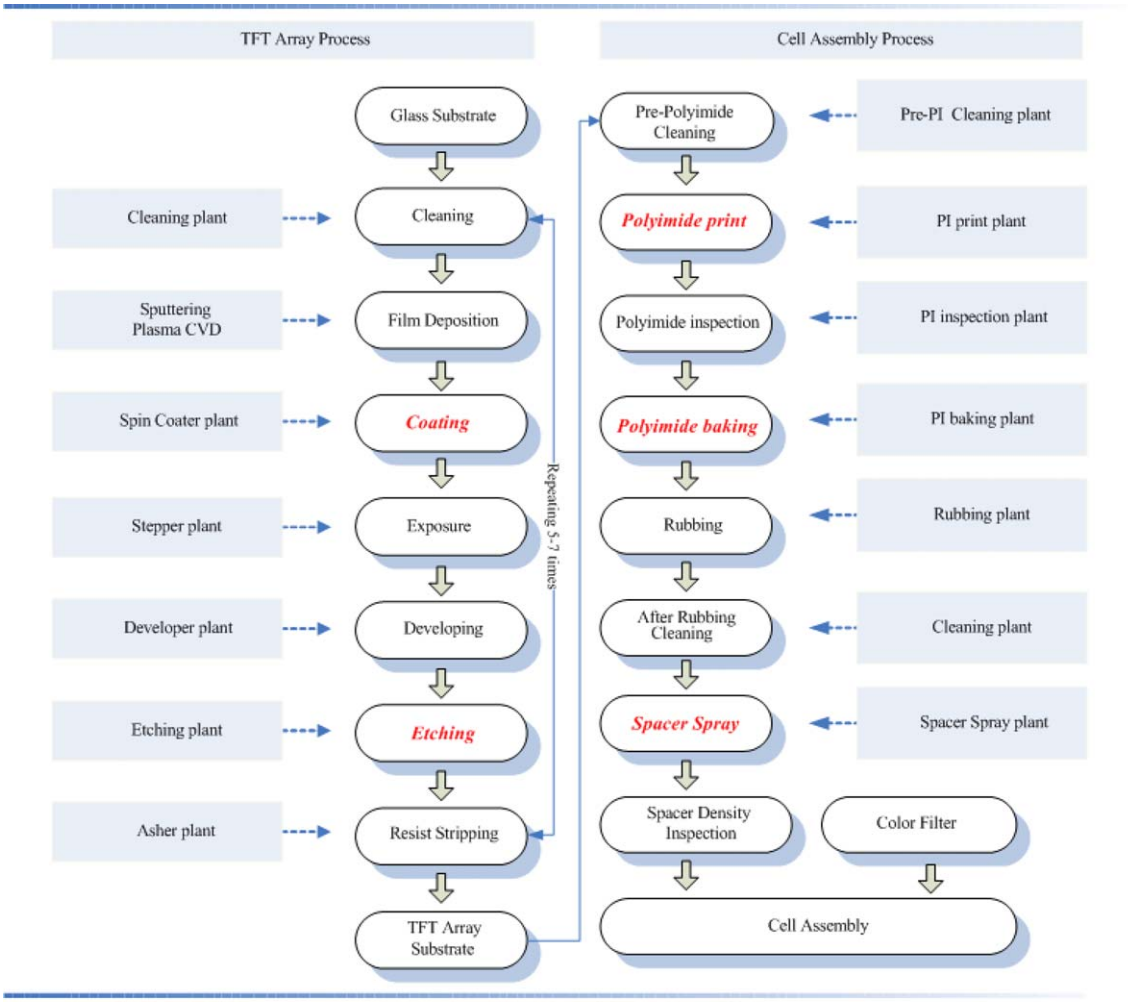

** "**CVD**" and "**PI**" are the abbreviations of "Chemical Vapor Deposition" and "Polyimide", respectively.

Fig. 1. The TFT-LCD panel manufacturing process.

Table 1
Specifications for five CTQ characteristics of TFT-LCD panel manufacturing process

Stages	CTQ characteristics	Specifications
TFT array process	Photo-resist coating thickness	20,000 Å ± 2000 Å[a]
	Etching path width	20 μm ± 1 μm[b]
Cell assembly process	Polyimide thickness (PI thickness)	500 Å ± 100 Å
	PI baking thickness	300 Å ± 50 Å
	Density of spacer spray	160 ± 60 pcs[c]

[a] 1 Å = 10^{-10} m.
[b] 1 μm = 10^{-6} m.
[c] pcs = bead/cm^2.

the main raw material of *TFT array process* is the glass substrate which must be processed 5–7 times through cleaning, coating, exposure, developing, etching, and stripping, etc. *Cell assembly process* is a special stage in TFT-LCD panel manufacturing process, in which two components, *color filter* and *TFT array substrate* will be processed through cleaning, alignment-layer printing, rubbing and so forth. Then, *color filters* will be added on the seal and be appended to *TFT array substrate* as shown in Fig. 1. After assembling, the liquid crystal will be injected into the spacer. *Module assembly process* is the final stage of TFT-LCD panel manufacturing process where the TFT-LCD panels passed from liquid crystal process are assembled with all the necessary parts such as black lights, driver IC, and printed wiring board (PWB), to complete the final TFT-LCD product. Among them, both TFT *array* and *cell assembly processes* are regarded as the most critical stages that can affect TFT-LCD panel quality. As manufacturing process variations arise in *TFT array* or *cell assembly process*, process faults such as the non-uniformities of panel thickness, spacer density, or etching path width occur frequently. Moreover, *module assembly process* or the function of final panels will be impacted to cause lower process performance and higher cost. Thus, process quality excellence is very important in *TFT array* and *cell assembly processes*. Hence, they are key issues in this paper. In Fig. 1, the sub-process with bold italicized words, referred to as critical-to-quality (CTQ) characteristic, is required to meet specified specification.

In *TFT array process* (or stage), photo-resist coating thickness and etching path width are two CTQ characteristics (sub-processes) which determine whether the quality of following sub-processes meets the requirement. In addition, the uniformities of PI thickness, PI baking thickness and density of spacer spray in *cell assembly process* are three CTQ characteristics. If they are non-uniform, then either the following module cannot be assembled or the color aberration of panel display is significantly impacted. The corresponding specifications for these five CTQ characteristics of TFT-LCD panel manufacturing process are shown as Table 1.

Obviously, all of the five CTQ characteristics belong to nominal-the-best type listed in Table 1. Based on Bothe [1], Huang et al. [13] and Chen et al. [7], the customers will be satisfied with the product only when all quality characteristics of a multi-characteristic product meet the specification requirements. However, research on TFT-LCD panel manufacturing process is comparatively scarce and incomplete, and most studies focus only on production technology and process quality assessment [14]. Process quality improvement methods and models were seldom proposed for poorer processes. Consequently, in this paper, the capability assessment model of TFT-LCD panel manufacturing process is provided to measure whether the process meets the requirements based on the five mentioned CTQ characteristics. Furthermore, MAIC approach of Six Sigma, proposed by Ham and Lee [11], is used to find the CTQ characteristics that make TFT-LCD panel unqualified or incapable. Finally, it will assist panel manufacturers in enhancing process quality and performance.

2. The process quality index for TFT-LCD panel

As described above, TFT *array* and *cell assembly* stages possess two and three CTQ characteristics, respectively. These CTQ characteristics are all nominal-the-best type with symmetric tolerance as displayed in Table 1. Chen et al. [7] have already developed a nominal-the-best multi-characteristic product capability analysis (MCPCA) chart for S_{pk} to monitor and assess the performance of an entire product and all process characteristics simultaneously. Nevertheless, according to Boyles [3], the index S_{pk} is defined based on process yield and is irrelevant to target value (T) for normally distributed process. There is a one-to-one mathematical relationship between S_{pk} and process yield. However, it fails to assess the process loss. To solve the problem, Chan et al. [4] have pointed out that the index C_{pm} can reflect the process loss and how the process center deviates from the target value. This paper employs this process quality index C_{pm} for responding process yield

and process expectation loss at the same time. Besides, based on Govaerts [10], we have process yield Yield% $\geqslant 2\Phi(3C_{\mathrm{pm}}) - 1$ when C_{pm} is sufficiently large. Since TFT-LCD panel manufacturing process includes five CTQ characteristics, the index $C_{\mathrm{pm}j}$ of jth CTQ characteristic can be written as following:

$$C_{\mathrm{pm}j} = \frac{\mathrm{USL}_j - \mathrm{LSL}_j}{6\sqrt{\sigma_j^2 + (\mu_j - T_j)^2}} = \frac{d_j}{3\sqrt{\sigma_j^2 + (\mu_j - T_j)^2}}, \quad (2.1)$$

where j represents jth CTQ characteristic in Table 1, $j = 1,\ldots,5$, and USL_j is the upper specification limit of jth CTQ characteristic. LSL_j is the lower specification limit of jth CTQ characteristic. T_j represents process target value of jth CTQ characteristic. μ_j and σ_j denote process mean and process standard deviation of jth CTQ characteristic, respectively; $d_j = (\mathrm{USL}_j - \mathrm{LSL}_j)/2$ represents process tolerance of jth CTQ characteristic. Indeed, given $C_{\mathrm{pm}j} = c$, we have:

$$P_j \leqslant 2 - 2\Phi(3c), \quad (2.2)$$

$$\frac{|\mu_j - T_j|}{d_j} \leqslant \frac{1}{3c}, \quad (2.3)$$

where P_j represents the non-conforming rate of jth CTQ characteristic. Φ is a cumulative probability function of standard normal distribution, and $|\mu_j - T_j|/d_j$ denotes the departure ratio of process tolerance from target value for jth CTQ characteristic. The larger the index $C_{\mathrm{pm}j}$ value (c) implies that the smaller the $|\mu_j - T_j|/d_j$ and the process non-conforming rate. Since all TFT-LCD panel manufacturing sub-processes are mutually dependent, based on Bothe [1], the relationship between non-conforming rates of entire TFT-LCD panel (P) and five individual CTQ characteristics (P_j) is

$$\mathrm{Max}\{P_1,\ldots,P_5\} \leqslant P \leqslant \sum_{j=1}^{5} P_j. \quad (2.4)$$

Based on Eqs. (2.2) and (2.4), the relationship between the non-conforming rates of entire TFT-LCD panel (P) and individual process quality index ($C_{\mathrm{pm}j}$) can be derived as following:

$$P \leqslant \sum_{j=1}^{5} P_j \leqslant \sum_{j=1}^{5} [2 - 2\Phi(3C_{\mathrm{pm}j})]. \quad (2.5)$$

According to Eq. (2.5), the entire process quality index (C_{pm}), which can reflect the non-conforming rate of entire TFT-LCD panel, is defined as below

$$C_{\mathrm{pm}} = \frac{1}{3}\Phi^{-1}\left\{1 - \sum_{j=1}^{5}[1 - \Phi(3C_{\mathrm{pm}j})]\right\}. \quad (2.6)$$

By Eq. (2.6), clearly, the relation between the entire non-conforming rate (P) and the entire process quality index (C_{pm}) is

$$P \leqslant 2 - 2\Phi(3C_{\mathrm{pm}}). \quad (2.7)$$

Based on Chen et al. [6], Huang et al. [13] and Chen et al. [7], when the entire process capability of TFT-LCD panel is required to be at a specified level, the individual process capabilities of all five CTQ characteristics must be better than the required standard for the entire product. For example, assuming the entire process quality index value $C_{\mathrm{pm}} = v$ is given, we have

$$C_{\mathrm{pm}} = \frac{1}{3}\Phi^{-1}\left\{1 - \sum_{j=1}^{5}[1 - \Phi(3C_{\mathrm{pm}j})]\right\} = v. \quad (2.8)$$

When the preset minimum values of individual process quality index ($C_{\mathrm{pm}j}$) are equal and refer to as w (i.e., $C_{\mathrm{pm}j} = w$), the critical value (w) for individual process quality index can be obtained by solving Eq. (2.8) as following:

$$w = \frac{1}{3}\Phi^{-1}\left[\frac{\Phi(3v) + 4}{5}\right]. \quad (2.9)$$

Table 2 displays various commonly used C_{pm} values, the corresponding $C_{\mathrm{pm}j}$ values and non-conforming rates. For an entire TFT-LCD panel manufacturing process with five CTQ characteristics, each individual

Table 2
Various C_{pm} values versus corresponding $C_{\mathrm{pm}j}$ values and non-conforming rates

C_{pm} (v)	Non-conforming rate (%)	$C_{\mathrm{pm}j}$ (w)	Non-conforming rate (%)
1.0	0.26997961	1.153	0.05399592
1.1	0.09668483	1.243	0.01933697
1.2	0.03182172	1.333	0.00636434
1.3	0.00961927	1.425	0.00192385
1.4	0.00266915	1.517	0.00053383
1.5	0.00067953	1.610	0.00013591
1.6	0.00015867	1.704	0.00003173
1.7	0.00003397	1.799	0.00000679
1.8	0.00000666	1.894	0.00000133
1.9	0.00000120	1.989	0.00000024
2.0	0.00000020	2.085	0.00000004

process capability (or quality) for the five characteristics should exceed w ($C_{pmj} \geqslant w$), thus, the entire process capability of TFT-LCD panel can be guaranteed to be v at least (i.e., $C_{pm} \geqslant v$). For instance, when $w = 1.153$ for all five characteristics, then the entire process capability value (v) can exceed 1.000.

3. Four phases of the Six Sigma approach

So far, the literature on quality assessment of TFT-LCD panel manufacturing process was comparatively scarce and incomplete. Some scholars and engineers only proposed the assessment approaches of process quality and production technology, but seldom provided improvement methods for the process quality [14]. Since the early 1900s, Six Sigma has been launched in service industries and manufacturing processes using statistical tools and techniques. It has been proven to be successful in reducing costs and cycle times, eliminating defects, raising customer satisfaction, and significantly increasing profitability [21]. Therefore, in this paper, Six Sigma quality improvement of the TFT-LCD panel through the MAIC approach, proposed by Ham and Lee [11] will be presented. The MAIC approach is divided into four core phases defined as (1) *Measure phase*: a review of measurement system types and the CTQ characteristics is included. The nature and properties of data collection must be thoroughly understood by TFT-LCD panel manufacturers. (2) *Analyze phase*: specific statistical methods and quality control tools are used to analyze and find out the critical information that is important to explaining the number of defects. (3) *Improve phase*: the critical factors that cause problems are discovered. The improvement actions will be taken for solving critical problems. (4) *Control phase*: the processes that create the product or service are controlled and monitored continuously in order to ensure that the problem will not occur again. The details of the MAIC approach in this paper are described as below.

3.1. Measure phase

To measure the quality and performance for TFT-LCD panel manufacturing process, the five CTQ characteristics of an entire TFT-LCD panel and their corresponding individual indices C_{pmj} have been completely introduced and discussed in the preceding section. Based on these concepts, a process assessment model will be developed to judge whether the process quality of each individual CTQ characteristic meets the requirement. Moreover, unqualified CTQ characteristics (or sub-processes) will be analyzed to find out the critical factors (or assignable causes). Next, the corrected action will be taken for improving the process quality of the entire TFT-LCD panel.

Since there are five CTQ characteristics in the TFT-LCD panel manufacturing process and each individual CTQ characteristic is nominal-the-best type with symmetric tolerance, in this paper we combine the approaches of Chen et al. [6], Deleryd and Vännman [9] and Sung et al. [19] with index C_{pmj} to develop a new process capability control chart, called "multi-characteristic product capability analysis chart – MPCAC/C_{pm}", for assessing the process capability of the TFT-LCD panel. This control chart can transform the specification tolerance (LSL_j, T_j, USL_j) of each individual CTQ characteristic into $(-1, 0, 1)$ by standardized procedure and describe all characteristics in one single chart to assess the process capabilities of these characteristics simultaneously. The procedure is presented as below. First of all, given $C_{pmj} = w$, we have

$$\frac{1}{\sqrt{(\sigma_j/d_j)^2 + [(\mu_j - T_j)/d_j]^2}} = 3w, \quad j = 1, \ldots, 5. \tag{3.1}$$

Moreover, the accurate index (Q_{aj}) and precision index (Q_{pj}) for jth CTQ characteristic are defined as following, respectively:

$$Q_{aj} = \frac{\mu_j - T_j}{d_j}, \quad j = 1, \ldots, 5, \tag{3.2}$$

$$Q_{pj} = \frac{\sigma_j}{d_j}, \quad j = 1, \ldots, 5. \tag{3.3}$$

Obviously, the smaller the Q_{aj} and Q_{pj} values imply that the higher the process accuracy and process precision. Based on Eq. (3.2), if $\mu_j < T_j$, then $Q_{aj} < 0$; if $\mu_j > T_j$, then $Q_{aj} > 0$; and if $\mu_j = T_j$, then $Q_{aj} = 0$ (the process is just on process target). Since the individual CTQ characteristic is nominal-the-best type with symmetric tolerance, if $\mu_j = LSL_j$, then $Q_{aj} = -1$; and if $\mu_j = USL_j$, then $Q_{aj} = 1$. Thus, the specification tolerance of jth CTQ characteristic can be transformed from (LSL_j, T_j, USL_j) into $(-1, 0, 1)$. If the indices Q_{aj} and Q_{pj} are represented as the X-axis and Y-axis, respectively, Eq. (3.1) can be rewritten as

$$X^2 + Y^2 = r^2, \tag{3.4}$$

where $X = Q_{aj}$, $Y = Q_{pj}$ and $r = 1/(3w)$ is the radius of a circle (or contour curve). The contour curve with bold line for $C_{pmj} = w$ can be drawn and shown as Fig. 2. Clearly, the smaller the Q_{aj} and Q_{pj} values imply the smaller the r value and the larger the index C_{pmj} value. In addition, the higher the process accuracy and process precision imply the better the process capability of jth characteristic.

As proposed by Chen et al. [6], Motorola's Six Sigma quality level means that process standard deviation is $\sigma = d/6$ with a 1.5σ shift. That is, $Q_{pj} = 1/6$ and $|Q_{aj}| \leqslant 0.25$. Assuming that entire process quality for TFT-LCD panel is required to meet Six Sigma quality level, the corresponding entire process capability should

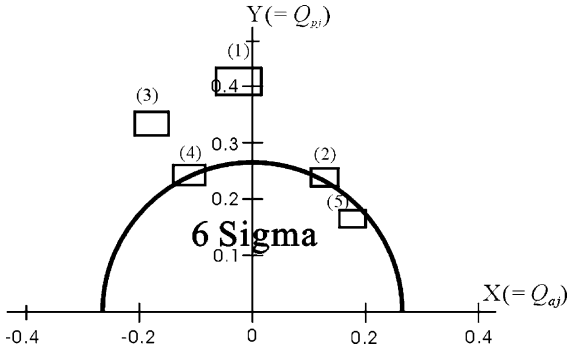

Fig. 2. Multi-characteristic product capability analysis chart (MPCAC/C_{pm}).

exceed 1.109 (i.e., $C_{pm} \geqslant 1.109$). The TFT-LCD panel manufacturing process possesses five CTQ characteristics, according to Eq. (2.9), the corresponding lower limit value of individual index C_{pmj} value can be calculated to be 1.251 (i.e., $C_{pmj} \geqslant 1.251$). For the same reason, the C_{pm} values of various quality levels such as 5 Sigma, 4 Sigma and so forth as well as the corresponding C_{pmj} values can be attained (shown in Table 3).

Moreover, combining the individual C_{pmj} value ($w = 1.251$) listed in Table 3 with equation $r = 1/(3w)$, the radius $r = 0.267$ is attained and the corresponding bold contour curve (or control limit) can be drawn as Fig. 2. Q_{aj} and Q_{pj} represent the axis-X (horizontal axis) and axis-Y (vertical axis), respectively. Obviously, a coordinate point (X, Y) represents an individual CTQ process (or characteristic). When the corresponding coordinate point of each individual CTQ characteristic is plotted on MPCAC/C_{pm}, we can judge the process quality condition by the corresponding location on the control chart. However, as the parameters μ_j and σ_j for the indices Q_{aj} and Q_{pj} are unknown, they must be estimated by sampling. Cheng [8] and Huang et al. [13] indicated some practitioners and scholars simply employed the point estimates of the indices to determine whether a process capability meets the requirement. Those approaches are not objective since sampling errors are neglected [16]. Hence, in this paper we replace a coordinate point (Q_{aj}, Q_{pj}) with its joint confidence region for assessing TFT-LCD panel process quality. The approach is described as following.

Table 3
The C_{pm} values of various quality levels and the corresponding C_{pmj} values

Quality level	C_{pm} value	C_{pmj} value
6 Sigma	$\geqslant$1.109	$\geqslant$1.251
5 Sigma	$\geqslant$0.925	$\geqslant$1.088
4 Sigma	$\geqslant$0.740	$\geqslant$0.930
3 Sigma	$\geqslant$0.555	$\geqslant$0.781

The $\overline{X} - S^2$ control chart is applied to monitor the mean and variability of TFT-LCD panel manufacturing process in this study. Assume that m sub-samples of size n are taken from an 'in-control' TFT-LCD panel manufacturing process. The estimators of Q_{aj} and Q_{pj} can be defined as $\hat{Q}_{aj} = (\overline{\overline{X}}_j - T_j)/d_j$ and $\hat{Q}_{pj} = \sqrt{\overline{S_j^2}}/d_j$, where $\overline{\overline{X}}_j = \sum_{i=1}^{m} \overline{X}_{ji}/m$ is the average of all sub-sample means for jth CTQ characteristic. $\overline{S}_j^2 = \sum_{i=1}^{m} S_{ji}^2/m$ is the average of all sub-sample variances for jth CTQ characteristic. $\overline{X}_{ji} = \sum_{k=1}^{n} X_{jik}/n$ is ith sub-sample mean. $S_{ji}^2 = \sum_{k=1}^{n} (X_{jik} - \overline{X}_{ji})^2/(n-1)$ is ith sub-sample variances. Next, we mimic Deleryd and Vännman [9] and Sung et al. [19], thus, the joint confidence region is a rectangle constructed by the $100(1-\alpha)\%$ confidence interval of Q_{aj}, $[\hat{Q}_{aj} \pm T_{\alpha/4}(v)\,\hat{Q}_{pj}/\sqrt{mn}]$ and the $100(1-\alpha)\%$ confidence interval of Q_{pj}, $\left[\sqrt{v\hat{Q}_{pj}^2/\chi_{\alpha/4}^2(v)},\ \sqrt{v\hat{Q}_{pj}^2/\chi_{1-\alpha/4}^2(v)}\right]$, where degrees of freedom $v = m(n-1)$, $T_{\alpha/4}(v)$ is an upper $\alpha/4$ percentile of T distribution with v degrees of freedom. $\chi_{1-\alpha/4}^2(v)$ and $\chi_{\alpha/4}^2(v)$ are upper $1-\alpha/4$ and $\alpha/4$ percentiles of χ^2-distribution with v degrees of freedom, respectively. Consequently, the four corner points of the joint confidence region for coordinate (Q_{aj}, Q_{pj}) can be represented as following in clockwise order from upper-right coordinate to upper-left coordinate:

$$\text{Upper-right: } \left[\hat{Q}_{aj} + T_{\alpha/4}(v)\hat{Q}_{pj}/\sqrt{mn}, \sqrt{v\hat{Q}_{pj}^2/\chi_{1-\alpha/4}^2(v)}\right], \tag{3.5}$$

$$\text{Bottom-right: } \left[\hat{Q}_{aj} + T_{\alpha/4}(v)\hat{Q}_{pj}/\sqrt{mn}, \sqrt{v\hat{Q}_{pj}^2/\chi_{\alpha/4}^2(v)}\right], \tag{3.6}$$

$$\text{Bottom-left: } \left[\hat{Q}_{aj} - T_{\alpha/4}(v)\hat{Q}_{pj}/\sqrt{mn}, \sqrt{v\hat{Q}_{pj}^2/\chi_{\alpha/4}^2(v)}\right], \tag{3.7}$$

$$\text{Upper-left: } \left[\hat{Q}_{aj} - T_{\alpha/4}(v)\hat{Q}_{pj}/\sqrt{mn}, \sqrt{v\hat{Q}_{pj}^2/\chi_{1-\alpha/4}^2(v)}\right]. \tag{3.8}$$

As we previously mentioned, when the entire process quality of the TFT-LCD panel is required to meet Six Sigma quality level, all process quality index values for individual CTQ characteristics should exceed 1.251 (i.e., $C_{pmj} \geqslant 1.251$). Thus, the contour curve with radius $r = 0.267$ for $C_{pmj} = 1.251$ can be drawn and shown as Fig. 2. Since computer technique has been rapidly developed, Montgomery [15] indicated that the larger sample number for a continuous random variable can be conveniently collected. Based on this

concept, 30 sub-samples of size 11 are taken from each CTQ characteristic (or sub-process) of TFT-LCD panel manufacturing process. Thus, $\overline{\overline{X}}_j$ and $\overline{S_j^2}$ can be calculated at significance level $\alpha = 0.05$. Furthermore, $\hat{Q}_{aj}$, $\hat{Q}_{pj}$ and the four coordinate points of joint confidence region for jth CTQ characteristic can also be obtained (see Table 4). Finally, the joint confidence regions of the five CTQ characteristics are plotted on MPCAC/C_{pm} as shown in Fig. 2. The TFT-LCD panel manufacturing process meets Six Sigma quality level when all joint confidence regions are located within or on the control limit. Conversely, the CTQ processes are unqualified and must be upgraded when some of the joint confidence regions are located outside the control limit. The process capability of entire TFT-LCD panel is incapable at the same time.

3.2. Analyze phase

First of all, MPCAC/C_{pm} was employed to discover unqualified CTQ characteristics. As a result, three CTQ characteristics, etching path width, PI baking thickness and density of spacer spray, meet Six Sigma quality level among five CTQ characteristics in Fig. 2. Besides, two CTQ characteristics—photo-resist coating thickness and PI thickness—did not meet Six Sigma quality level, in which the quality level of photo-resist coating thickness was the worst. Obviously, we knew large process variation (or lack of process precision) has occurred and resulted in photo-resist coating process capability incapable by the location of corresponding joint confidence region on MPCAC/C_{pm}. Therefore, in this paper photo-resist coating process was selected as the first improvement project for TFT-LCD panel manufacturing process. Next, we used some statistical tools and quality methods like cause-and-effect (or fish-bone) diagram, brainstorming and so forth to find out the critical factors rendering photo-resist coating process incapable. In practice, when enterprises in Taiwan carry out quality activities, the cause-and-effect diagram is a necessary and useful tool. Besides, Syrcos [20] used the cause-and-effect diagram to study and analyze the casting density. In this study, to analyze and discover the critical factors for making photo-resist coating process incapable (or lack of process precision), the cause-and-effect diagram (shown in Fig. 3) would be an improvement tool of TFT-LCD panel manufacturing process project.

Table 4
Estimated index values for five CTQ characteristics and corresponding coordinates

CTQ characteristics	Specification	Unit	$\hat{Q}_{aj}$	$\hat{Q}_{pj}$	Upper-right	Bottom-right	Bottom-left	Upper-left
Photo-resist coating thickness	20000 ± 2000	Å	−0.03	0.41	[0.03, 0.45]	[0.03, 0.37]	[−0.08, 0.37]	[−0.08, 0.45]
Etching path width	20 ± 1	μm	0.13	0.24	[0.16, 0.26]	[0.16, 0.22]	[0.10, 0.22]	[0.10, 0.26]
PI thickness	500 ± 100	Å	−0.19	0.33	[−0.14, 0.36]	[−0.14, 0.30]	[−0.23, 0.30]	[−0.23, 0.36]
PI baking thickness	300 ± 50	Å	−0.11	0.24	[−0.07, 0.26]	[−0.07, 0.22]	[−0.14, 0.22]	[−0.14, 0.26]
Density of spacer spray	160 ± 60	pcs	0.18	0.17	[0.20, 0.18]	[0.20, 0.15]	[0.15, 0.15]	[0.15, 018]

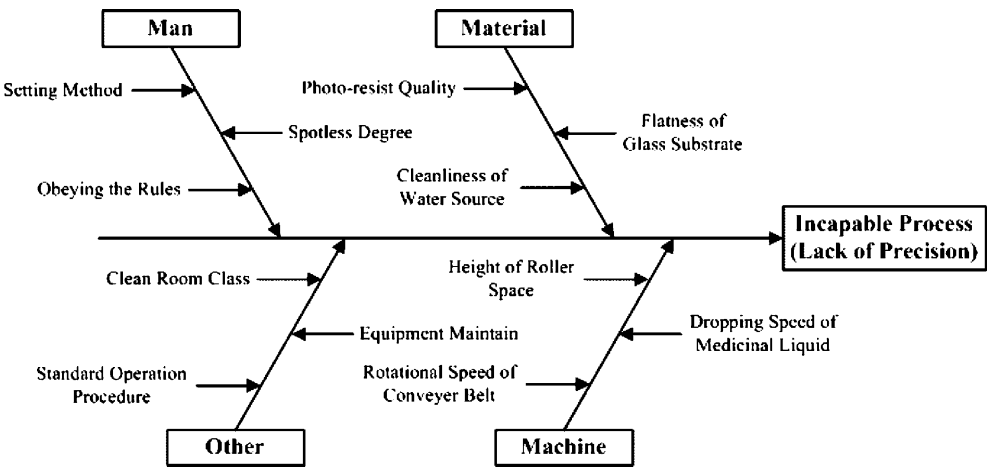

Fig. 3. The cause-and-effect diagram for rendering photo-resist coating process incapable.

After a thorough discussion of the cause-and-effect diagram shown in Fig. 3 with Six Sigma project manager and process engineers, three machine parameter settings (i.e., critical factors)—height of roller space, dropping speed of medicinal liquid and rotational speed of conveyer belt—were identified as major causes which made process capability of photo-resist coating process for TFT-LCD panel incapable. Herein, roller space that is too high or too low can make photo-resist coating thickness either too thick or too thin. Thus, the exposure process quality will be impacted. Besides, photo-resist coating thickness will be non-uniform when dropping speed of medicinal liquid is too fast or too slow. Finally, rotational speed of conveyer belt that is too fast or too slow will affect baking time of the panels in the oven after finishing photo-resist coating. Moreover, the photo-resist coating process quality will deteriorate. In other words, the setting values of three aforementioned machine parameters will directly impact the precision of photo-resist coating process. They can even render TFT-LCD panel manufacturing process incapable or unqualified. Consequently, project manager and process engineers decided to actively focus their improvement plan and study on these three machine parameters and discover the optimal parameter settings. Among them, although the height of roller space was a critical factor which impacts coating thickness uniform, based on previously experimented results, the process precision of TFT-LCD panel was the most stable when the height of roller space was preset to be 2.3 mm. Besides, when rotational speed of conveyer belt was preset to be 625 cm/min, process stability was also the best. Thus, the dropping speed of medicinal liquid would be further discussed and researched in the following section to improve the capability and performance for TFT-LCD panel manufacturing process.

3.3. Improve phase

In the analysis of above mentioned MPCAC/C_{pm} approach, the result showed that the capability and precision of photo-resist coating process was not satisfactory. Then, the cause-and-effect diagram and brainstorming were used to find out the critical factor (i.e., dropping speed of medicinal liquid) rendering photo-resist coating process incapable. In this phase, Hartley's homogeneity test [12,17] and joint confidence intervals [5] were conducted to determine the optimal parameter setting of the dropping speed of medicinal liquid. It was divided into three factor levels—35, 40 and 45 drops/min in this study. At the same time, n_i samples were selected at each level. Then, $\hat{C}_{pmi} = (USL - LSL)/\{6[S_i^2 + (\bar{X}_i - T)^2]^{1/2}\}$ can be calculated, where i represents ith factor level ($i = 1, 2, 3$). To test H_0: $C_{pm1} = C_{pm2} = C_{pm3}$ against the alternative H_1: Not all C_{pmi} are equal ($i = 1, 2, 3$), this paper follows *Hartley's test* [12,17] to employ F_{max} as a testing statistic, which was defined as

$$F_{max} = \frac{\min\left\{\hat{C}_{pm1}^2, \hat{C}_{pm2}^2, \hat{C}_{pm3}^2\right\}}{\max\left\{\hat{C}_{pm1}^2, \hat{C}_{pm2}^2, \hat{C}_{pm3}^2\right\}}. \tag{3.9}$$

When H_0 is true, then

$$F_{max} = \frac{\max\left\{\left(C_{pm1}/\hat{C}_{pm1}\right)^2, \left(C_{pm2}/\hat{C}_{pm2}\right)^2, \left(C_{pm3}/\hat{C}_{pm3}\right)^2\right\}}{\min\left\{\left(C_{pm1}/\hat{C}_{pm1}\right)^2, \left(C_{pm2}/\hat{C}_{pm2}\right)^2, \left(C_{pm3}/\hat{C}_{pm3}\right)^2\right\}}. \tag{3.10}$$

Since $\left(C_{pmi}/\hat{C}_{pmi}\right)^2 \sim \chi^2_{v_i}/v_i$ ($i = 1, 2, 3$) [2,5], where $v_i = n_i \times [(1 + \lambda_i/n_i)^2/(1 + 2\lambda_i/n_i)]$ and $\lambda_i = n_i \times (\mu_i - T)^2/\sigma_i^2$, then $F_{max} \sim F_{max[3,\bar{v}-1]}$ (see Appendix 1 for details). Consequently, F_{max} is a *Hartley's* F_{max} distribution with 3 and $\bar{v} - 1$ degrees of freedom, where $\bar{v} = \sum_{i=1}^{3} v_i/3$ and 3 represents the number of selected factor level. v_i denotes the degree of freedom of ith factor level.

The null hypothesis H_0 is rejected at α level if $F_{max} > C_0$, where C_0 is a critical value which is satisfied with $P(F_{max} > C_0 | H_0 \text{ is true}) = \alpha$. Furthermore, we checked the table of Hartley's F_{max} distribution [17] based on α value, 3 and $\bar{v} - 1$ degrees of freedom, C_0 could be attained. Assuming that null hypothesis H_0 is rejected, that means there is a significant difference among the three levels. Next, to distinguish the process quality and performance of one level from other levels, $C_2^3 = 3$ kinds of multiple comparisons—called the confidence intervals for C_{pm1}/C_{pm2}, C_{pm1}/C_{pm3} and C_{pm2}/C_{pm3}, were constructed and calculated. Conversely, the null hypothesis H_0 is not rejected if $F_{max} < C_0$. That means no significantly better level exists in dropping speed of medicinal liquid. At this time, the experiment of another level for dropping speed of medicinal liquid must be performed and analyzed. Moreover, since samples had been collected at each level, the three estimates—$\hat{C}_{pm1}$, $\hat{C}_{pm2}$ and $\hat{C}_{pm3}$—were calculated as 1.005, 1.289 and 1.150, respectively. Next, we obtained $F_{max[3,29]} = 0.9907/0.2911 = 3.425$ by Eq. (3.9). Clearly, H_0 was rejected at $\alpha = 0.05$ level since $F_{max[3,29]} > C_0 = 2.4$. That meant there was a significant difference among the three factor levels. Finally, to investigate and find out the best factor level, the confidence intervals of C_{pm1}/C_{pm2}, C_{pm1}/C_{pm3} and C_{pm2}/C_{pm3} [5] were calculated at 95% confidence level and the results were shown in Table 5.

Table 5
The 95% confidence intervals of the index ratios for three dropping speeds of medicinal liquid

	Lower confidence limit	Upper confidence limit	Results
C_{pm1}/C_{pm2}	0.1199	0.7201	$C_{pm1} < C_{pm2}$
C_{pm1}/C_{pm3}	0.3114	1.8670	$C_{pm1} = C_{pm3}$
C_{pm2}/C_{pm3}	1.0598	6.3636	$C_{pm2} > C_{pm3}$

According to the results of the final column in Table 5, obviously, C_{pm2} value was significantly larger than C_{pm1} and C_{pm3} values. Hence, when dropping speed of medicinal liquid was set to be 40 drops/min, the process performance was best and the process capability could be upgraded to around 1.289. That means the TFT-LCD panel manufacturing process meets Six Sigma quality level.

3.4. Control phase

As preceding experiments showed, when the dropping speed of medicinal liquid was set to be 40 drops/min and other process parameters remained unchanged, the process precision and capability for TFT-LCD panel were the best. Thus, TFT-LCD panel manufacturing process would be preset to the combination of these factor levels in the future. According to Spiring [18], after the Improve Phase of Six Sigma has been finished, the process is generally stable. Thus, $\overline{C}_{pm}$ control chart is suitable for this section. Moreover, based on Boyles [2], $\overline{C}_{pm}$ control chart was developed and employed to monitor the process quality and presented as following. First of all, m sub-samples of size n were taken from the TFT-LCD panel manufacturing process. Thus, parametric estimators are described as below. $\overline{X}_l = \sum_{k=1}^{n} X_{lk}/n$ denotes lth sub-sample mean and $S_l^2 = \sum_{k=1}^{n} (X_{lk} - \overline{X}_l)^2/(n-1)$ represent lth sub-sample variance. Thus, the average of all sub-sample means is $\overline{\overline{X}} = \sum_{l=1}^{m} \overline{X}_l/m$, and the average of all sub-sample variances is $\overline{S^2} = \sum_{l=1}^{m} S_l^2/m$. Furthermore, the process quality index value, $\overline{C}_{pml} = 1/\left\{3\sqrt{(S_l/d_l)^2 + [(\overline{X}_l - T_l)/d_l]^2}\right\}$, for lth sub-sample as well as the average of quality index values for all sub-samples, $\overline{\overline{C}}_{pm} = \sum_{l=1}^{m} \overline{C}_{pml}/m$, could be obtained.

In fact, based on Boyles [2] and Chen and Chen [5], $v \times (C_{pm}^2/\hat{C}_{pm}^2)$ approximately follows Chi-square distribution (χ^2) with degrees of freedom v, where $v = mn \times [(1+\lambda/mn)^2/(1+2\lambda/mn)]$ and $\lambda = mn \times (\mu - T)^2/\sigma^2$. Estimator of the unknown parameter λ is defined by $\bar{\lambda} = mn \times (\overline{\overline{X}} - T)^2/\overline{S^2}$, and estimated degree of freedom is $\bar{v} = mn \times [(1+\bar{\lambda}/mn)^2/(1+2\bar{\lambda}/mn)]$. Hence, the upper and lower control limits for $\overline{C}_{pm}$ control chart could be easily derived by mimicking S^2 control chart. They are presented as following:

$$\mathrm{UCL}_{\overline{C}_{pm}} = I_1 \times \overline{\overline{C}}_{pm}, \tag{3.11}$$

$$\mathrm{CL}_{\overline{C}_{pm}} = \overline{\overline{C}}_{pm}, \tag{3.12}$$

$$\mathrm{LCL}_{\overline{C}_{pm}} = I_2 \times \overline{\overline{C}}_{pm}, \tag{3.13}$$

where I_1 and I_2 are the functions of $\chi^2_{1-\alpha/2}(\bar{v})$ and $\chi^2_{\alpha/2}(\bar{v})$, respectively, and $\chi^2_{1-\alpha/2}(\bar{v})$ and $\chi^2_{\alpha/2}(\bar{v})$ are upper $1-\alpha/2$ and $\alpha/2$ percentiles of χ^2-distribution with $\bar{v}$ degrees of freedom, respectively:

$$I_1 = \sqrt{mn \times \left\{\left[1 + \left(\overline{\overline{X}} - T\right)^2 \Big/ \overline{S^2}\right]^2 \Big/ \left[1 + 2\left(\overline{\overline{X}} - T\right)^2 \Big/ \overline{S^2}\right]\right\} \Big/ \chi^2_{1-\alpha/2}(\bar{v})}, \tag{3.14}$$

$$I_2 = \sqrt{mn \times \left\{\left[1 + \left(\overline{\overline{X}} - T\right)^2 \Big/ \overline{S^2}\right]^2 \Big/ \left[1 + 2\left(\overline{\overline{X}} - T\right)^2 \Big/ \overline{S^2}\right]\right\} \Big/ \chi^2_{\alpha/2}(\bar{v})}. \tag{3.15}$$

In practice, based on Eqs. (3.11)–(3.15), $\overline{C}_{pm}$ control chart is constructed for monitoring and controlling the process quality. For instance, if $T = 100$ and $d = 2$ are given and 30 sub-samples of size 11 are collected, then $\overline{\overline{X}} = 98$, $\overline{S^2} = 1$ and $\overline{\overline{C}}_{pm} = 1.2$ are calculated. Thus, $I_1 = 1.05$ and $I_2 = 0.96$ are attained at $\alpha = 0.05$ level, and the upper and lower control limits of $\overline{C}_{pm}$ are calculated as 1.258 and 1.148, respectively. To sustain the improvement results in TFT-LCD panel manufacturing process, this control chart is recommended for the panel manufacturers.

4. Conclusions

Since the TFT-LCD panel manufacturing process is quite complicated, the possibility of committing mistakes is very high. In addition, the earlier and later manufacturing sub-processes for TFT-LCD panel are mutually dependent, thus, quality defects in a sub-process or a stage can impact the later stages or the function of final products and the cost will increase. Based on the concepts, five CTQ characteristics in TFT-LCD panel manufacturing process are identified and summarized, and the entire process quality index (C_{pm}) and individual CTQ index (C_{pmj}) are defined according to Chen et al. [7] in this paper. Moreover, we combine the approach of Chen et al. [6], Deleryd and Vännman [9] and Sung et al. [19] with index C_{pmj} to develop a new process capability control chart, called MPCAC/C_{pm}, for assessing whether the process capability of TFT-LCD panel meets requirement. Next, MAIC approach of Six Sigma, proposed by Ham and Lee [11], is used to discover the CTQ characteristics making TFT-LCD panel unqualified or incapable and assists panel manufacturers in enhancing process quality and performance. In a word, this paper provides a C_{pm}-based methodology for solving TFT-LCD panel process problems and the empirical-based results can be sufficiently applied to implement the other project of Six Sigma. Besides, the CTQ characteristics are assumed to be normally distributed throughout this paper. The non-normal processes or characteristics are not discussed in this study. It will be an interesting research issue in the future.

Appendix 1

By Hartley's test, to test H_0: $\sigma_1^2 = \sigma_2^2 = \sigma_3^2$ against the alternative H_1: not all σ_i^2 are equal ($i = 1, 2, 3$), we obtain the test statistic $F_{\max[3,\bar{\nu}-1]} = \frac{S^2_{\max}}{S^2_{\min}} = \frac{\max\{S_1^2, S_2^2, S_3^2\}}{\min\{S_1^2, S_2^2, S_3^2\}}$, when H_0 is true, then

$$F_{\max[3,\bar{\nu}-1]} = \frac{\max\left\{\left(\frac{\nu_1 S_1^2}{\sigma_1^2}\right)/\nu_1, \left(\frac{\nu_2 S_2^2}{\sigma_2^2}\right)/\nu_2, \left(\frac{\nu_3 S_3^2}{\sigma_3^2}\right)/\nu_3\right\}}{\min\left\{\left(\frac{\nu_1 S_1^2}{\sigma_1^2}\right)/\nu_1, \left(\frac{\nu_2 S_2^2}{\sigma_2^2}\right)/\nu_2, \left(\frac{\nu_3 S_3^2}{\sigma_3^2}\right)/\nu_3\right\}} = \frac{\max\left\{\chi^2_{\nu_1}/\nu_1, \chi^2_{\nu_2}/\nu_2, \chi^2_{\nu_3}/\nu_3\right\}}{\min\left\{\chi^2_{\nu_1}/\nu_1, \chi^2_{\nu_2}/\nu_2, \chi^2_{\nu_3}/\nu_3\right\}}, \quad (1)$$

where $\bar{\nu} = \sum_{i=1}^{3} \nu_i/3$.

This paper follows Hartley's method to employ a testing statistic $F_{\max}$ to test H_0: $C_{\mathrm{pm1}} = C_{\mathrm{pm2}} = C_{\mathrm{pm3}}$ against the alternative H_1: not all $C_{\mathrm{pm}i}$ are equal ($i = 1, 2, 3$). $F_{\max}$ is defined as $F_{\max} = \frac{\min\left\{\hat{C}^2_{\mathrm{pm1}}, \hat{C}^2_{\mathrm{pm2}}, \hat{C}^2_{\mathrm{pm3}}\right\}}{\max\left\{\hat{C}^2_{\mathrm{pm1}}, \hat{C}^2_{\mathrm{pm2}}, \hat{C}^2_{\mathrm{pm3}}\right\}}$, when H_0 is true, then

$$F_{\max} = \frac{\max\left\{\left(C_{\mathrm{pm1}}/\hat{C}_{\mathrm{pm1}}\right)^2, \left(C_{\mathrm{pm2}}/\hat{C}_{\mathrm{pm2}}\right)^2, \left(C_{\mathrm{pm3}}/\hat{C}_{\mathrm{pm3}}\right)^2\right\}}{\min\left\{\left(C_{\mathrm{pm1}}/\hat{C}_{\mathrm{pm1}}\right)^2, \left(C_{\mathrm{pm2}}/\hat{C}_{\mathrm{pm2}}\right)^2, \left(C_{\mathrm{pm3}}/\hat{C}_{\mathrm{pm3}}\right)^2\right\}},$$

since $\left(C_{\mathrm{pm}i}/\hat{C}_{\mathrm{pm}i}\right)^2 \sim \chi^2_{\nu_i}/\nu_i$ $(i = 1, 2, 3)$, we have

$$F_{\max} = \frac{\max\left\{\chi^2_{\nu_1}/\nu_1, \chi^2_{\nu_2}/\nu_2, \chi^2_{\nu_3}/\nu_3\right\}}{\min\left\{\chi^2_{\nu_1}/\nu_1, \chi^2_{\nu_2}/\nu_2, \chi^2_{\nu_3}/\nu_3\right\}}. \quad (2)$$

As previously derived, Eq. (1) is equal to Eq. (2). We have $F_{\max} \sim F_{\max[3,\bar{\nu}-1]}$.

References

[1] Bothe DR. A capability study for an entire product. ASQC Qual Cong Tran 1992;46:172–8.

[2] Boyles RA. The Taguchi capability index. J Qual Technol 1991;23:17–26.

[3] Boyles RA. Process capability with asymmetric tolerances. Commun Stat: Comput Simul 1994;23:615–43.

[4] Chan LK, Cheng SW, Spiring FA. A new measure of process capability: C_{pm}. J Qual Technol 1988;20(3):162–75.

[5] Chen JP, Chen KS. Comparison of two process capabilities using C_{pm}. J Qual Technol 2004;36(3):329–35.

[6] Chen KS, Pearn WL, Lin PC. Capability measures for processes with multiple characteristics. Qual Reliab Eng Int 2003;19:101–10.

[7] Chen KS, Huang ML, Li RK. Process capability analysis for an entire product. Int J Prod Res 2001;39(17):4077–87.

[8] Cheng SW. Practical implementation of the process capability indices. Qual Eng 1994–1995;7:239–59.

[9] Deleryd M, Vännman K. Process capability plots—a quality improvement tool. Qual Reliab Eng Int 1999; 15(3):213–27.

[10] Govaerts B. Private communication to Kotz S; 1994.

[11] Ham CH, Lee YH. Intelligent integrated plant operation system for Six Sigma. Annu Rev Control 2002;26:27–43.

[12] Hartley HO. The maximum F-ratio as a shortcut test for heterogeneity of variance. Biometrika 1950;37(3/4):308–12.

[13] Huang ML, Chen KS, Hung YH. Integrated process capability analysis with an application in backlight. Micro Reliab 2002;42:2009–14.

[14] Lin JT, Chen TL, Huang CC. A hierarchy planning model for TFT-LCD production chan. Int J Electron Busi Manag 2004;2(1):59–68.

[15] Montgomery DC. Introduction to statistical quality control. 4th ed. New York: Wiley; 2001.

[16] Pearn WL, Chen KS. One-sided capability indices C_{pu} and C_{pl}: decision making with sample information. Int J Qual Reliab Manag 2002;19(3):221–45.

[17] Pearson ES, Hartley HO. Biometrika Tables for Statisticians. 3rd ed. Biometrika Trustees; 1966.

[18] Spiring FA. Process capability: a total quality management tool. Tot Qual Manag 1995;23(1):21–33.

[19] Sung WP, Chen KS, Go CG. Analytical method of process capability for steel. Int J Adv Manuf Technol 2002;20: 480–484.

[20] Syrcos GP. Die casting process optimization using Taguchi method. J Mater Process Technol 2003;135:68–74.

[21] Tong JPC, Tsung F, Yen BPC. A DMAIC approach to printed circuit board quality improvement. Int J Adv Manuf Technol 2004;23:523–31.